Analysis and Research on the Load Braking Process and Motion Posture Characteristics of Crane Lifting Equipment

Deyang Liu*

Zhuhai Branch, Guangdong Institute of Special Equipment Inspection and Research, Zhuhai 519002, China

Abstract: In the process of lifting heavy objects with cranes, the shortcomings of current conventional detection methods were analyzed in terms of applicability, safety, and reliability. In response to the safety risks associated with the braking process and motion posture characteristics of crane lifting equipment, this paper proposes a method for detecting the braking process and motion posture of crane lifting equipment. By collecting data on the braking process and motion posture, and using Kalman filtering method for filtering and fusion, accurate data can be obtained; Analyze the waveform characteristics of experimental data and integrate them in the time domain to calculate the value of brake sliding displacement has improved the accuracy and efficiency of detection results and reduced detection costs. These analysis features and calculation results provide strong support for the comprehensive evaluation of the braking performance of cranes, which helps to promote the standardization of operation and improve overall operational safety, and ensure the safe use of lifting machinery and equipment.

Keywords: Crane, Lifting Load, Braking Process, Movement Posture

DOI: 10.57237/j.se.2024.04.002

1 Introduction

As an indispensable equipment in industrial and mining enterprises, ports and harbours, roads and bridges and other critical areas, the safety performance of cranes is of utmost importance. Among them, the brake slippage displacement is regarded as one of the key indicators for evaluating its safety. TSG 51-2023 "Technical Regulations for Safety of Hoisting Machinery" in the crane brake slippage displacement to do the relevant requirements, in practice to ensure that the crane brake slippage displacement in the stipulated permissible range of the crane is crucial. Therefore, strict control and monitoring of the crane's brake slippage displacement, to ensure the safety of industrial production and lifting and handling is of great significance.

In the crane brake slippage displacement detection method, visual error, pulling the line and high-speed image range distance is limited and the safety of the equipment itself is a threat, the laser measurement method of the spreader load shaking unstable defects and other issues, scholars have also carried out a lot of research. The pull-wire detection method proposed by Zhuhai Inspection Institute has the limitation of detection range and the

Funding: Science and Technology Project of Guangdong Provincial Administration for Market Regulation «Research on Stability Analysis of Crane Operation and Fault Characteristics and Diagnostic Techniques of Key Components in Transmission System» (Project Nos: 2025CT11);
Zhuhai Social Development Science and Technology Plan Project (Project Nos: 2420004000343);
Guangdong Special Equipment Testing and Research Institute Technology Project (Project Nos: 2023JD-2-02, 2024-1-02).

*Corresponding author: Deyang Liu, 1427368630@qq.com

Received: 5 August 2024; Accepted: 11 September 2024; Published Online: 26 October 2024 http://www.sciandeng.com

safety risk problem under the rated load in practical application [1, 15]; Gu Huiyong's research focuses on the detector of crane sliding displacement to achieve the sliding displacement that can be accurately measured under the rated load [2]; Wang Jun et al. provide an in-depth analysis of the current detection of braking sliding displacement and discuss the innovative design and development of the detection The innovative design and development of detection methods [3, 11]; Wang Lichao focuses on the spreader motion attitude detection of truck cranes, and solves the motion state by calculating the motion attitude of the spreader [4, 14]; Wang Linan's technical team from Hefei University of Technology has conducted an in-depth study of three-dimensional motion attitude fusion technology, and achieved a significant improvement in the fusion accuracy [5]; Wang Xiaoyi has explored the method of brake slide displacement detection of cranes using Hall sensors [6]. According to the principle of work to build a closed-loop monitoring system, you can accurately obtain the crane braking slide displacement. To address the problems of the above methods this paper uses a combination of acceleration sensors, gyroscope sensors and magnetometers to accurately capture the instantaneous sudden changes in acceleration on the Z-axis through advanced algorithms, and at the same time, with the help of gyroscope sensors to calibrate the deflection angle errors that may occur during the braking process, and the use of magnetometers to assist in identifying and judging these deflection angles, which significantly enhances the accuracy and reliability of the measurement results of braking downward displacement detection. This significantly improves the accuracy and reliability of the measurement results of the brake downward displacement detection.

2 Detection Scheme

This paper designs a portable detection scheme based on the brake sliding displacement of the crane as the research object. The core of this solution lies in the fusion of detection technologies from three types of sensors. Through continuous optimization and improvement, it aims to significantly enhance the measurement accuracy and reliability of sensors, ensuring more accurate and reliable measurement data for practical applications, thereby effectively supporting the safe operation and performance evaluation of cranes.

2.1 Testing and Measurement Process

The detection scheme for the braking process and motion posture of the crane is shown in Figure 1. The acceleration sensor, gyroscope sensor, and magnetometer use magnetic attraction to vertically attach the data acquisition device to the bottom of the lifting load. Firstly, confirm the accuracy of the detection results by monitoring the current; Secondly, use wireless trigger buttons to remotely control and collect the values of its motion speed and deflection angle, and process the filtered data; Then, further data fusion is performed to calculate a more accurate estimation of the deflection angle; Finally, this detection method effectively reduces the impact of wind load and wire rope shaking in the lifting system on the measurement results, thereby significantly improving the accuracy of the detection.

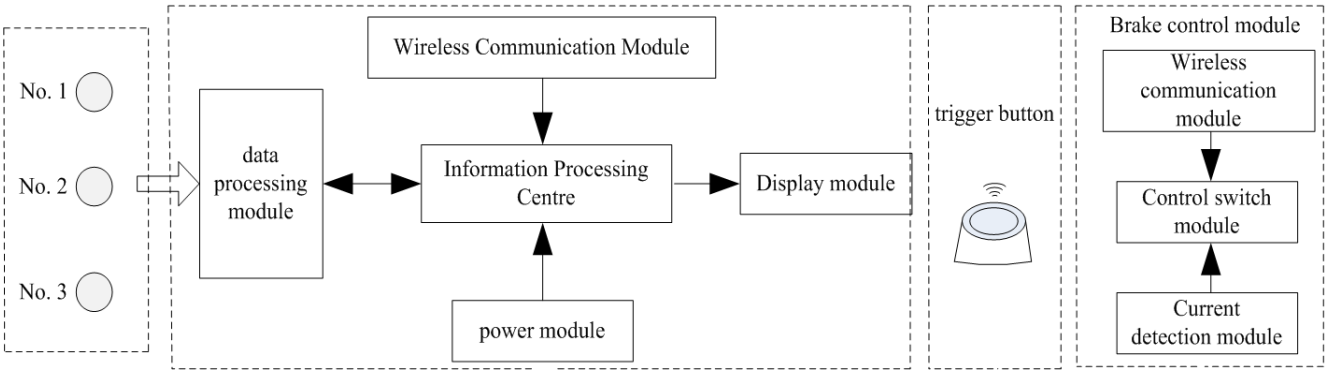

Figure 1 Detection and measurement process of motion posture during crane braking process

Accurate control of data collection through manual triggering control. The data acquisition module is fixed on the lifting device of the crane, and the control module is connected in series in the emergency stop control circuit of the crane to achieve the detection function of the crane braking process. In order to further improve the accuracy

of control, the control module schematic diagram 2 specifically introduces a current transformer detection method, effectively avoiding errors caused by misjudgment. The wireless trigger button sends control commands, ensuring that the braking and data collection of the crane can be accurately synchronized at the same time, thereby significantly reducing the errors in the detection data.

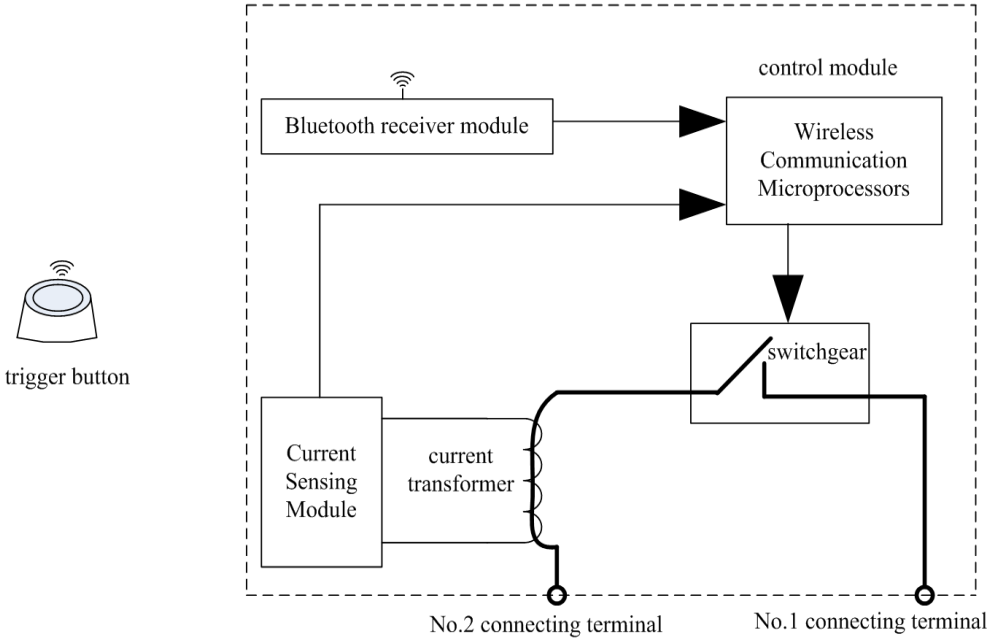

Figure 2 Schematic diagram of brake control module

This article uses acceleration sensors, gyroscope sensors, and magnetometers in the data acquisition module. To provide real-time, high-precision performance data related to roll angle, pitch angle, and heading angle in dynamic and static environments for collecting and detecting data. The performance indicators of its related sensors are shown in Table 1.

Table 1 Performance Parameters of Detection and Measurement Sensors

Sensor type / serial number	Acceleration sensors		Gyro Sensor		magnetometer	
	index	parameter	index	parameter	index	parameter
1	Range (?sec)	±500	Range (?sec)	±16	Heading accuracy	1 °
2	Zerobias repeatability (deg/s)	0.025mg	Zero bias repeatability (deg/s)	0.9mg	repeatability	0.1 °
3	Zero-bias instability (deg/h)	3.7mg	Zero-bias instability (deg/h)	0.5mg	measuring range	0~360 °
4	Random angle wanderin (?sqrt (Hz))	0.3	Random angle wanderin (?sqrt (Hz))	0.05	acquisition frequency	50Hz
5	resolution ratio (?s)	0.0175	resolution ratio (?s)	0.000488	resolution ratio	0.1 °
Index (25 ℃)	roll angle	Pitch angle	Relative heading angle	unit	Start delay	≤50ms
output value range	±180	±90	±180	.	voltage	9~36V
resolution ratio	0.01	0.01	0.01	.	current	45mA
Static accuracy	±0.3	±0.3	/	.	Storage range	-55~+125 ℃
static error	/	/	±0.3	?h	operation temperature	-40~+85 ℃
Rotational Accumulated Error	/	/	±0.3	?360 °	weights	45g

In the lifting system of lifting machinery, there are six degrees of freedom for the lifting device load to move and rotate in the X, Y, and Z directions. The factors that affect changes in the lifting angle include flexible shaking of the steel wire rope in the lifting system, wind load, uneven force distribution, and eccentric torsion. In Figure 3, the

braking sliding attitude motion model [7] shows that the rated load belongs to the six degrees of freedom of multi-body system dynamics, and two coordinate systems are established based on the center O of the hoisting pulley and the Earth's magnetic field OB. In the research on the detection and measurement of sliding displacement with braking, factors such as wind load swing, steel wire rope elastic vibration, and brake inertia can have varying degrees of impact on the detection and measurement results of the lifting equipment load. In order to improve the accuracy of detection and measurement results; The processing and fusion of deflection angle and braking speed data are optimized and improved to obtain accurate braking slip.

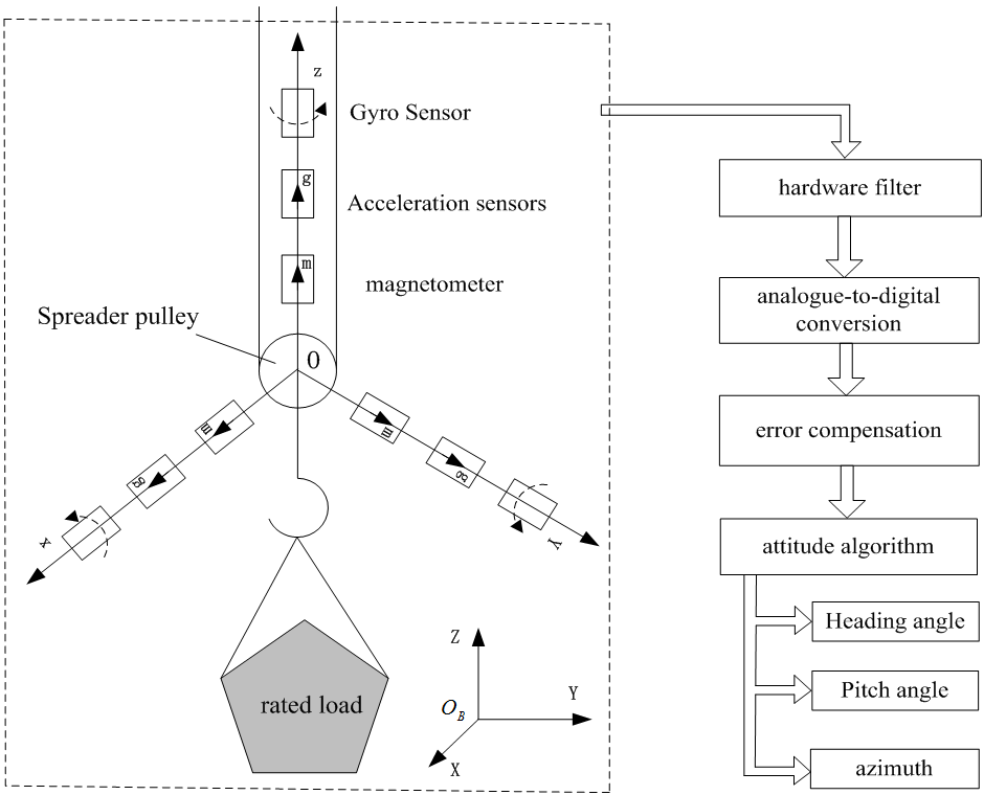

Figure 3 Brake sliding posture motion model

When considering the motion characteristics of crane lifting equipment and the potential impact of wind loads on it, it is necessary to analyze multiple factors comprehensively [10], Set the rated load of the lifting device to m, The posture angle of the lifting device load is θ, The rope length at the moment of braking is l_0, The speed of rope length change is $\dot{x}$, gravitational acceleration g, The elastic coefficient of the steel wire rope is k, Wire rope length x, The acceleration of rope length change is $\ddot{x}$, Load angular velocity $\dot{\theta}$, Load swing angular acceleration $\ddot{\theta}$, wind load Q, Establish a sliding displacement model of the coordinate system based on the rectangular x-direction of the steel wire rope.

(1) The load on the lifting device in the vertical downward direction is decomposed into $m\cos\theta$

(2) The length of the elastic change of the steel wire rope is $x - l_0$

(3) The kinetic energy generated by the movement of the lifting device and its load in the tangential direction $E_{k1} = \frac{1}{2}m\dot{x}^2$, Vertical kinetic energy: $E_{k2} = \frac{1}{2}m\left(x\dot{\theta}\right)^2$, The sum of lifting energy is: $T = E_k = \frac{1}{2}m\dot{x}^2 + \frac{1}{2}m\left(x\dot{\theta}\right)^2$

(4) The lifting potential energy is the sum of the potential energy V of the lifting device load and the elastic potential energy E_p of the steel wire rope. The formula is:

$$E = V + E_P = -mgx\cos\theta + \frac{1}{2}k\left(x - l_0\right)^2 \quad (1)$$

The simplified Lagrangian operator is obtained by subtracting the system potential energy E_k from the system potential energy E:

$$L = T - E = \frac{1}{2}m\dot{x}^2 + \frac{1}{2}mx^2\dot{\theta}^2 + mgx\cos\theta - \frac{1}{2}kx^2 + kxl_0 - \frac{1}{2}kl_0^2 \quad (2)$$

From the formula $\frac{d}{dt}\left(\frac{\partial T}{\partial \dot{q}_i}\right) - \frac{\partial T}{\partial q_i} = Q_i\left(i = 1, 2, \cdots\right)$, $\left(q_i, \dot{q}_i\right)$ -Generalised coordinates of the prime system, i -Number of degrees of freedom of the plasma system, Q_i -Generalized Inertial Force of Particle System, Inference leads to Lagrange's nonlinear equation:

(1) When evaluating the impact of wind on lifting equipment, a Lagrange equation is established in the direction of force x on the steel wire rope to quantify the effect of non force $Q^*\sin\theta$ generated by wind loads. This non influential force is described through the Lagrange operator L and requires first-order and second-order differentiation of the coordinate particles at a certain point on the length x of the steel wire rope. After a series of calculations and processing, the following mathematical equation was obtained:

$$\begin{cases} \frac{\partial L}{\partial \dot{x}} = m\dot{x} \\ \frac{d}{dt}\left(\frac{\partial L}{\partial \dot{x}}\right) = m\ddot{x} \\ \frac{\partial L}{\partial x} = mx\dot{\theta}^2 + mg\cos\theta - kx + kl_0 \\ \frac{d}{dt}\left(\frac{\partial L}{\partial \dot{x}}\right) - \frac{\partial L}{\partial x} = m\ddot{x} - mx\dot{\theta}^2 - mg\cos\theta + kx - kl_0 = Q^*\sin\theta \end{cases} \quad (3)$$

Formula (3), simplified as the first Lagrangian equation:

$$\frac{d^2x}{dt^2} = g\cos\theta + x\dot{\theta}^2 + \frac{k\left(l_0 - x\right)}{m} + \frac{Q^*\sin\theta}{m} \quad (4)$$

(2) When considering the motion characteristics of the lifting device, the inclination angle θ of the lifting device is selected as the reference to construct the spatial coordinate system of the Lagrange equation [10]. Simplify this model by ignoring other possible influencing factors and focusing on the direct impact of wind on the load of lifting equipment. The effect of wind load on the load of the lifting device is not constant, and it will change accordingly with the variation of the angular velocity of the lifting device. In other words, the force of wind on the inclined lifting device load can be expressed as the product of the projected area of the lifting device load object in the wind direction and the wind direction force at that time. This product constitutes the wind load force $F_\theta = Q^*\mathrm{sign}\left(\dot{\theta}\right)^*\cos\theta$. Then there are:

$$\begin{cases} \frac{\partial L}{\partial \dot{\theta}} = mx^2\dot{\theta} \\ \frac{d}{dt}\left(\frac{\partial L}{\partial \dot{\theta}}\right) = 2mx\dot{x}\dot{\theta} + mx^2\ddot{\theta} \\ \frac{\partial L}{\partial \theta} = -mgx\sin\theta \\ \frac{d}{dt}\left(\frac{\partial L}{\partial \dot{\theta}}\right) - \frac{\partial L}{\partial \theta} = 2mx\dot{x}\dot{\theta} + mx^2\ddot{\theta} + mgx\sin\theta = Q^*sign\left(\dot{\theta}\right)^*\cos\theta \end{cases} \quad (5)$$

Simplify the second Lagrangian equation of the available lifting system:

$$\frac{d^2\theta}{dt^2} = -\frac{2\dot{x}}{x}\dot{\theta} - \frac{g}{x}\sin\theta + \frac{Q^*sign\left(\dot{\theta}\right)^*\cos\theta}{mx^2} \quad (6)$$

After calculation and processing, the nonlinear dynamic equation of the crane lifting system can be obtained:

$$\begin{cases} \frac{d^2x}{dt^2} = g\cos\theta + x\dot{\theta}^2 + \frac{k\left(l_0 - x\right)}{m} + \frac{Q^*\sin\theta}{m} \\ \frac{d^2\theta}{dt^2} = -\frac{2\dot{x}}{x}\dot{\theta} - \frac{g}{x}\sin\theta + \frac{Q^*sign\left(\dot{\theta}\right)^*\cos\theta}{mx^2} \end{cases} \quad (7)$$

2.2 Data Filter Fusion

During the operation of a crane, its lifting system inevitably faces vibration and friction from the steel wire rope, strong winds in the external environment, and the impact of the brake at the moment of braking. In order to improve the accurate capture ability of the real-time motion posture of the lifting equipment load, this paper adopts data fusion technology to integrate and analyze the obtained raw data. This method effectively reduces the impact of external factors on system performance, thereby significantly improving the stability and reliability of the entire lifting system [8, 17, 18]. As shown in Figure 4.

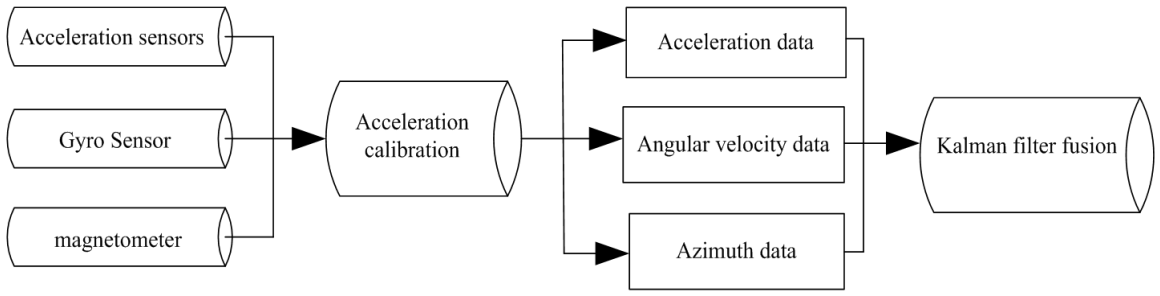

Figure 4 Processing Flow of Load Movement Data for Lifting Equipment

(1) To improve the accuracy of data collection, it is necessary to calibrate the accelerometer accurately. The accelerometer is greatly affected by linearity and needs to improve its linearity. This article uses the static six position method for calibration, and in the calibration model, it is necessary to consider the axial zero deviation of the three axes and the overall calibration of the scale factor coefficient. The calibration model for acceleration sensors is:

$$\begin{aligned} A_x &= B_x + S_x V_x + E_{xy} V_y + E_{xz} V_z \\ A_y &= B_y + E_{yx} V_x + S_y V_y + E_{yz} V_z \\ A_z &= B_z + E_{zx} V_x + E_{zy} V_y + S_z V_z \end{aligned} \tag{8}$$

Formula, $A_i (i = x、y、z)$ is the actual acceleration value on the x-axis、z-axis、y-axis, $B_i (i = x、y、z)$ is the zero bias of acceleration, $S_i (i = x、y、z)$ is the scaling factor, $E_{ij} (i = x、y、z, j = x、y、z, i \neq j)$ installation error coefficient, $V_i (i = x、y、z)$ is a voltage analog quantity.

Implementation plan: Collect static data from sensors X Y and Z up and down respectively, and calculate the average value of the voltage analog for measurement and calculation. Based on the error model of the acceleration sensor, the coefficient calculation formula is used to calculate the coefficients using the least squares method, and the sensor calibration error model formula is obtained.

(2) Calibration of acceleration sensors can improve measurement accuracy by applying Kalman filtering to the collected data in order to reduce measurement errors. The Kalman filtering method removes interference signals from the original data and obtains a smooth curve to estimate the target position. The Kalman filtering algorithm is used to estimate the state of the next moment, which requires continuous filtering updates, covariance calculation for the next update prediction, and continuous replacement calculation. In discrete linear systems, given initial values and data at each time step, the optimal state estimate of the system can be obtained.

(3) During the lifting process of a crane, due to inertia, the brake will momentarily shake, and under the elastic action of wind and steel wire rope, it will tilt and shake. These factors will cause significant errors in the detection results. In order to solve the above problems, this article cleverly uses a gyroscope sensor to accurately capture the change in tilt angle. The acceleration data during braking descent is deeply fused with the angle data measured by the gyroscope sensor. At the same time, the Kalman filtering algorithm is combined to remove abnormal data, correct the drift phenomenon of the gyroscope sensor, and improve the measurement effect.

2.3 Braking and Motion Attitude Algorithms

(1) Brake displacement

When calculating the braking sliding displacement during the lifting operation of a crane, acceleration data is collected, integrated to obtain the speed of the braking process, and then integrated to obtain the braking sliding displacement [9, 12].

The acceleration signal in the time domain is $a(t) = f(t) + B$, where B is the measurement error, $a(t)$ is the acceleration data, and $f(t)$ is the acceleration function over time t. The integral formula for velocity and displacement is shown in formula (9):

$$s(t) = \int v(t) d(t) = \iint f(t) d(t)(t) + \frac{1}{2} Bt + Et + K \tag{9}$$

Among them, $s(t)$ is the braking displacement, $v(t)$ is the braking sliding speed, E represents energy, and K is the stiffness of the system steel wire rope. In the process of integral calculation, the acceleration value of the $d(t)$

micro variable used to describe the change of variables is often accompanied by an error parameter B, which changes during continuous integration and can cause singular values in the calculation results, that is, outliers. To solve this problem, it is necessary to effectively suppress it during the calculation process. By using the Kalman filtering algorithm to remove abnormal data and integrating it in the time domain, accurate braking sliding displacement can be obtained [10, 13, 16, 19, 20].

(1) Space motion posture

Crane hoisting equipment requires precise control of its motion posture during braking, relying on gyroscope sensors, acceleration sensors, and magnetometers to collect numerical data. The gyroscope sensor measures angle, velocity and determines attitude, the accelerometer calculates attitude based on the direction angle, and the magnetometer determines attitude based on the projection of geomagnetic vectors. After data fusion, the motion posture of the lifting equipment is obtained, and then a posture motion model of the crane is constructed. Its posture motion equation:

$$\dot{q} = \frac{1}{2} E(q)\omega \tag{10}$$

In the above equation, q represents the quaternion pose, $q_0 \in R$ is the scalar part of quaternion q, and when q_0 is zero, the quaternion represents a three-dimensional spatial vector; If $\vec{q}_v = [q_1, q_2, q_3]^T \in R$ is the vector part of a quaternion and $\vec{q}_v$ is divided into a three-dimensional zero vector, then it degenerates into a real number; The angular velocity of the lifting device is ω, measured by a gyroscope sensor. The expression of spatial motion posture $E(q)$ is as follows:

$$E(q) = \begin{bmatrix} -\vec{q}_v^T \\ q_0 I + S(q_v) \end{bmatrix} \tag{11}$$

In formula (11), I is the third-order identity matrix of the scalar coefficients of quaternions; $S(q_v)$ represents the following opposition matrix:

$$S(q_v) = \begin{bmatrix} 0 & -q_3 & q_2 \\ q_3 & 0 & -q_1 \\ -q_2 & q_1 & 0 \end{bmatrix} \tag{12}$$

In formula (12), q_1, q_2, q_3 represents the three-dimensional spatial motion vectors of the X axis, Y axis, and Z axis, respectively.

Because the attitude calculation of the crane lifting equipment is closely related to the angular velocity ω, using accurate angular velocity to solve for a more accurate attitude estimation value $\hat{q}$. Due to the sensitivity of gyroscope sensors but their tendency to generate errors, while accelerometers and magnetometers have no cumulative errors but slow responses, complementary filters are used to fuse the data from these three sensors in the frequency spectrum, thereby improving measurement accuracy and system dynamic response. The formula obtained is:

$$\dot{\omega} = \omega_g + \left(K_p + \frac{K_I}{s}\right)\left(a(t) \times \omega_1 + \rho \times \omega_2\right) \tag{13}$$

In the formula, ω represents angular velocity, s represents complex frequency variable, $\dot{\omega}$ represents angular velocity change rate, i.e. angular acceleration, ω_g is the angular velocity measured by the gyroscope sensor, $a(t)$ represents acceleration measurement data, ω_1 represents theoretical output value of the acceleration sensor, ρ represents measurement data of the magnetometer, ω_2 represents theoretical calculation value of the magnetometer, K_p, K_I is greater than zero position related gain. After updating the posture of the quaternion motion of the lifting device, it can be concluded that:

$$\begin{bmatrix} q_0 \\ q_1 \\ q_2 \\ q_3 \end{bmatrix}_{t+\Delta t} = \begin{bmatrix} q_0 \\ q_1 \\ q_2 \\ q_3 \end{bmatrix}_t + \frac{\Delta t}{2} \begin{bmatrix} -\omega_x q_1 - \omega_y q_2 - \omega_z q_3 \\ \omega_x q_0 + \omega_z q_2 - \omega_y q_3 \\ \omega_y q_0 - \omega_z q_1 + \omega_x q_3 \\ \omega_z q_0 + \omega_y q_1 - \omega_x q_2 \end{bmatrix} \tag{14}$$

In formula (14), $\omega_x, \omega_y, \omega_z$ represents the angular velocity changes along the X-axis, Y-axis, and Z-axis in the three-dimensional motion space, respectively.

3 Experimental Analysis

When conducting experiments on the braking process and motion posture of crane hoisting equipment, the sampling frequency is set to 500 times per second under a fixed rated load state. The acceleration, angular velocity, and angle values of the entire crane braking experiment process are collected and saved on the X, Y, and Z axes, respectively, and their waveform characteristics are ana-

lyzed. The experimental results of the load movement process of the crane lifting device are shown in Figure 5.

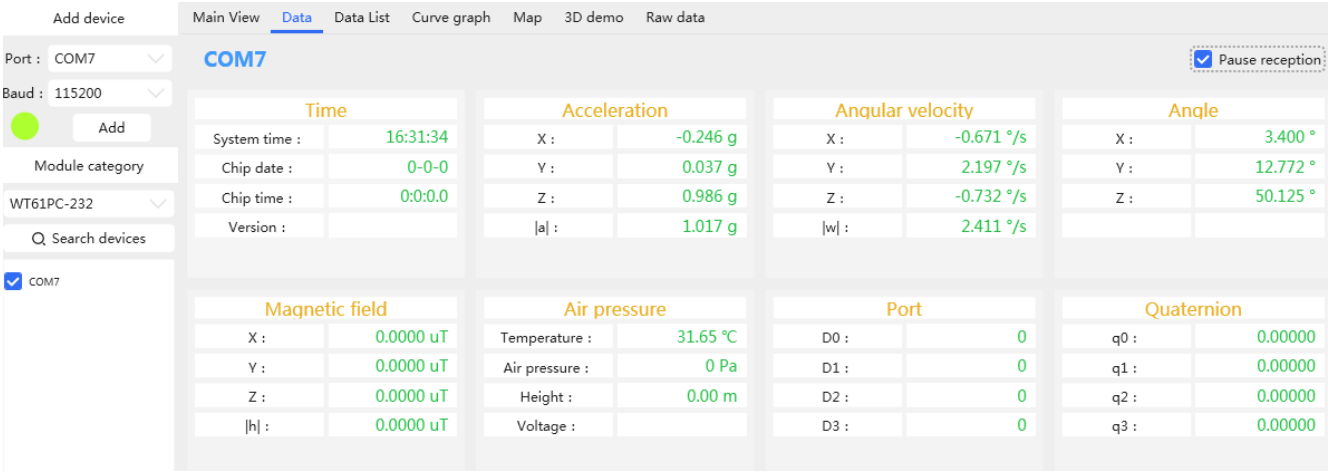

Figure 5 Experimental data display of crane spreader movement process

In Figure 6, when analyzing the acceleration waveform characteristics during the braking process of the crane in detail, it can be observed that the acceleration variation characteristics of the X and Y axes are mainly caused by external factors. The specific process of the crane's braking descent is clearly demonstrated through the acceleration variation characteristics of the Z-axis. This process starts with an initial acceleration descent, gradually transitions to a deceleration phase, and ultimately tends towards a stable stationary state.

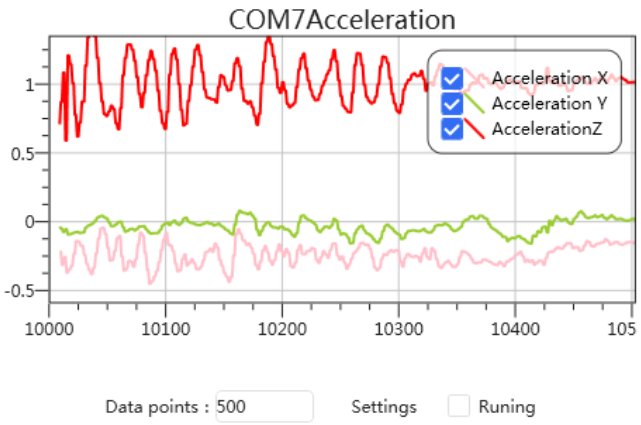

Figure 6 Analysis of Acceleration Waveform Characteristics during Braking Process

In Figure 7, the angular velocity variation characteristics of the entire braking process of the crane are shown, and a gyroscope sensor is used to collect the angular velocity. The following analysis focuses on the changes in angular velocity along the X, Y, and Z axes. The X-axis angular velocity mainly reflects the lateral or lateral movement of the lifting device, and can be used to analyze the lateral stability of the lifting device during braking; The Y-axis angular velocity mainly reflects the forward and backward movement of the lifting device. By analyzing the changes in the Y-axis angular velocity, the longitudinal stability of the lifting device during braking can be determined; The change in Z-axis angular velocity is usually related to the overall rotation of the lifting device. The lifting device rotates during braking, and the Z-axis angular velocity can help analyze the rotational stability of the lifting device during braking, preventing excessive rotation or unstable braking conditions.

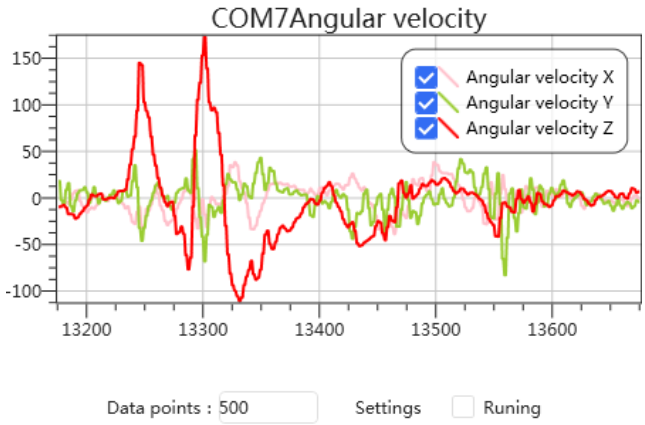

Figure 7 Analysis of Angular Velocity Waveform Characteristics during Braking Process

In Figure 8, the angle change characteristics of the entire braking process of the crane are shown, and a magnetometer is used to monitor the angle changes on the X, Y, and Z axes. The load of the lifting device deviates in the

X-axis direction, which may be caused by uneven ground, wind force, or imbalance between the lifting device and the load. Ensure the balance of the lifting device load, prevent swinging, and improve the accuracy of acceleration measurement results during the braking process; Due to uneven friction of the brake and other influencing factors such as ground slope, the load of the lifting device may tend to move forward or backward on the Y-axis; The rotation of the lifting device load in the Z-axis direction is caused by wind force, twisting of the lifting cable, or other factors. The angle change of the Z-axis can provide important information related to the stability of the lifting device and load.

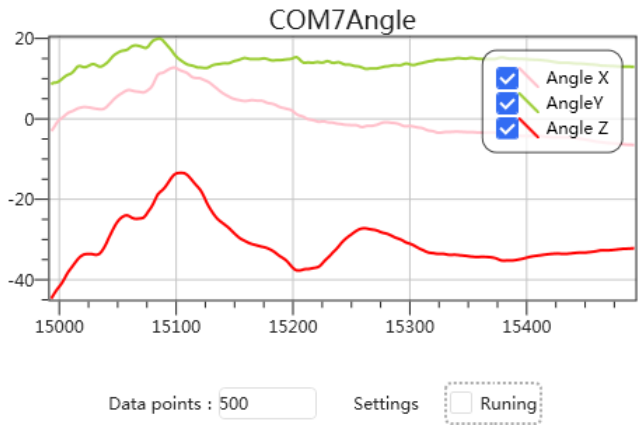

Figure 8 Analysis of Angle Waveform Characteristics during Braking Process

Statistical analysis was conducted on the braking process and motion posture data of the crane under no-load and loaded conditions. The changes in acceleration, angular velocity, and angle data are shown in Table 2. During the braking process, there is a slight shaking of the X-axis acceleration data to the left and right, a slight change in the Y-axis acceleration data to the front, and the Z-axis velocity value gradually increases downwards from the third line until it starts to decrease at the 18th line, until the lifting device moves in the opposite direction upwards. From the variation characteristics of the angular velocity and angle values of the X-axis, Y-axis, and Z-axis in Table 1, it can be concluded that the load of the lifting device is in a slightly unstable state during the entire braking process, with no significant change in the Z-axis angle, maintaining a vertical state. The load of the lifting device shows a sudden change in Z-axis acceleration value at the second line, resulting in an upward shaking state during the braking process; From the third line to the tenth line, the braking process is in a state where the downward acceleration value gradually increases; Starting from the 11th line, the acceleration value gradually decreases until the 17th line, and the speed reaches its maximum value at the 17th line; Then start decelerating at line 18 until it reaches a stable stationary state. By double integrating the acceleration values during the braking process in the time domain, the sliding displacement during braking is obtained.

Table 2 Statistical analysis of triggered braking process and motion attitude data

sequences	accelerations				angular velocity			angle		
	X (g)	Y (g)	Z (g)[0t]	Z (g)[5t]	X (°/s)	Y (°/s)	Z (°/s)	X (°)	Y (°)	Z (°)
1	0.363	0.492	-2.869	-7.597	51.392	-21.790	39.4851	11.124	15.271	1.89
2	0.375	0.429	3.174	1.551	83.191	-21.667	39.589	12.442	15.919	1.86
3	0.365	0.264	-16.846	-32.948	84.351	7.690	39.606	13.074	16.414	1.86
4	0.397	0.220	-84.839	-102.713	41.687	7.202	39.155	14.030	17.512	1.89
5	0.287	0.306	-119.629	-136.814	24.231	-12.573	37.430	14.535	18.040	1.88
6	0.252	0.372	-124.939	-184.627	26.367	-23.560	35.079	15.084	18.100	1.85
7	0.107	0.329	-161.377	-178.012	9.399	-57.678	32.393	15.776	17.814	1.90
8	0.105	0.200	-149.658	-161.658	12.451	-66.650	29.042	16.540	16.864	1.88
9	0.104	0.289	-198.364	-183.015	-90.332	-69.885	25.521	16.930	15.507	1.82
10	0.080	0.751	-217.224	-233.297	-79.651	-48.584	21.039	15.925	13.552	1.82
11	0.006	1.042	-180.298	-194.844	54.504	-18.005	16.677	15.463	12.420	1.83
12	-0.013	1.194	-141.479	-171.025	79.590	13.367	13.348	16.842	12.546	1.86
13	-0.110	1.437	-127.441	-139.109	7.202	31.250	8.355	18.847	14.024	1.87
14	-0.228	1.665	-135.315	-88.281	42.542	42.297	4.774	19.550	15.282	1.86
15	-0.365	2.068	-119.507	-62.385	105.957	47.607	2.637	21.297	16.397	1.86
16	-0.318	2.305	-22.583	-37.102	10.132	45.959	0.884	23.357	17.974	1.86
17	-0.246	2.001	39.490	-19.977	-20.447	40.283	1.055	23.307	18.946	1.89
18	-0.154	1.595	73.486	10.503	-30.640	29.541	2.241	22.742	19.748	1.86
19	-0.246	2.001	31.482	27.913	-20.447	40.283	1.577	23.055	19.380	1.89

By analyzing the triggering braking process and motion posture data in Table 3, it was found that there was a sig-

nificant difference in the acceleration results obtained in the braking test experiments with and without load Z (g) [0t]. Especially during the braking process of the crane, from the perspective of data changes, the braking acceleration curve of the lifting equipment under load is smoother, which significantly enhances the reliability of the experimental results. By comparing and analyzing the acceleration data of key points during the braking process in Table 2, it was found that the changing trend of the on load braking process is closer to the theoretical calculation results. Observing the data of each group, it can be clearly seen that the stability of the rated load detection results is good. Further comparison reveals that the error of the rated load measurement results is smaller compared to the no-load state, indicating higher accuracy of the measurement values.

Table 3 Comparison of measured acceleration data at key points of the braking process

Acceleration/time series / lifted load	Acceleration during braking process					
	2	**3**	**10**	**17**	**18**	**19**
theoretical value	1.973	-27.102	-237.422	-12.097	16.428	21.329
Z(g)[0t]	3.174	-16.846	-217.224	39.490	73.486	31.482
Z(g)[5t]	1.551	-32.948	-233.297	-19.977	10.503	27.913

4 Conclusion

This article designs a detection method for the braking process of cranes and the movement posture of lifting equipment loads, and analyzes the influencing factors. After filtering and fusing the acceleration, angular velocity, and angle data during the braking process to reduce the interference of data errors, their values can be obtained separately, and the waveform characteristics of the data can be analyzed. After detailed analysis through experiments, the characteristic changes and motion posture of the braking process of the crane hoist under load were obtained, which improved the accuracy of the calculation results of the sliding displacement of the crane during braking.

The entire detection system model design in this article still has limitations and urgently needs improvement. It should consider the operating state parameters when the small or large vehicle is in motion, so as to more comprehensively complete the detection and evaluation of the operating state of the lifting system. In addition, an external storage function is added to the motion parameters to facilitate the storage of a large amount of crane operation status detection data, as well as to facilitate future viewing, processing, and analysis of historical data.

References

[1] Lin Xiaoming, Li Chengzhi. Discussion on the detection method of crane brake sliding amount [J]. Mechanical and Electrical Engineering Technology, 2019, 48(11): 73-76.

[2] Gu Huiyong. Simple, efficient, and safe measurement method for the sliding amount of crane braking [J]. China Special Equipment Safety, 2016, 32(06): 18-21.

[3] Wang Jun, Gao Yan, Liu Yang. Analysis of the current situation and design prospects of crane brake sliding detection [J]. Brand and Standardization, 2014(16): 79-80.

[4] Wang Lichao. Research on Hook Motion Attitude Sensor Based on MEMS Technology [D]. Dalian: Dalian University of Technology, 2014.

[5] Wang Linan. Research on Finite Time Attitude Fusion Algorithm for quadcopter Drones [D]. Hefei: Hefei University of Technology, 2021.

[6] Wang Xiaoyi. Technical research on detecting the sliding amount of crane braking based on Hall sensors [J]. China Equipment Engineering, 2018, (24): 105-107.

[7] Wang Pengfei. Development of a Crane Braking Sliding Detection System Based on Dynamic Modeling and MEMS Technology [D]. Nanjing: Southeast University, 2016.

[8] Dai Wenjun. Research and Design of a Crane Braking Sliding Detection System [D]. Shanghai: Shanghai University of Applied Sciences, 2019.

[9] Wang Yanping. Analysis and Inspection of Brake Sliding of Crane Machinery [J]. Building Mechanization, 2013, 34 (06): 88-89+95.

[10] Liu Deyang, Yang Ningxiang, Li Qian, et al. Research on the Detection Method of Sliding Displacement of Crane Braking [J]. China Special Equipment Safety, 2024, 40 (03): 20-27.

[11] Xiao Haodi, Wu Fengqi, Liu Long, et al. Design of Crane Braking Sliding Measurement System Based on YOLOv5 [J]. Crane Transport Machinery, 2024, (03): 44-49.

[12] Qiu Guangbin. Economic Analysis of the Application of Crane Braking Sliding Detection System [J]. Modern Industrial Economics and Informatization, 2023, 13(12): 89-90+93.

[13] Xu Shengjun. Analysis of a Crane Braking Distance Measurement Method Based on Gravity Acceleration Sensor [J]. Market Regulation and Quality Technology Research, 2023, (03): 10-12.

[14] Zhu Fengjin, Lv Guizhi. Development of a Crane Brake Sliding Detection Instrument Based on Dynamic Displacement Detection [J]. Crane Transport Machinery, 2021, (16): 37-42.

[15] Zhao Tianyu, Lin Xiaoming, Guan Chengwen. Crane Brake Sliding Detection Instrument Based on Cable Sensor [J]. Western Special Equipment, 2021, 4(01): 19-24.

[16] Su Yuhang, Lin Xiaoming. Application of Acceleration Integration Method in Speed Measurement of Mechanical and Electrical Special Equipment [J]. Mechanical and Electrical Engineering Technology, 2020, 49(07): 160-162.

[17] Dai Wenjun, Ma Xianghua, Zhang Weikun. Research and Design of Crane Brake Sliding Detection Instrument Based on Load Status Monitoring [J]. Journal of Applied Technology, 2019, 19(01): 60-64.

[18] Zheng Jingxing, Wen Maotang, Yun Xiangyong. Design of a Crane Braking Trigger Signal Acquisition Device [J]. Crane Transport Machinery, 2023, (11): 79-84.

[19] Chen Hu, Qiu Jun. Measurement of Brake Sliding of Cranes Based on Accelerators [J]. China Special Equipment Safety, 2021, 37 (05): 22-25.

[20] Xie Xiaojuan, Lin Xiaoming, Liang Minjian. Design of Brake Sliding Test Device for Lifting Mechanism of Crane Machinery [J]. China Equipment Engineering, 2019, (19): 124-126.